



pH triggered smart organogel from DCDHF-Hydrazone molecular switch



Tawfik A. Khattab^{a, c, *}, Brylee David B. Tiu^b, Sonya Adas^a, Scott D. Bunge^a, Rigoberto C. Advincula^b

^a Department of Chemistry and Biochemistry, Kent State University, Kent, Ohio 44242, United States

^b Department of Macromolecular Science and Engineering, Case Western Reserve University Cleveland, Ohio 44106, United States

^c Dyeing, Printing and Auxiliaries Department, Textile Research Division, National Research Centre, Dokki, Cairo 12311, Egypt

ARTICLE INFO

Article history:

Received 30 December 2015

Received in revised form

22 March 2016

Accepted 23 March 2016

Available online 28 March 2016

Keywords:

DCDHF-Hydrazone

Molecular switch

pH-responsive

Smart organogel

Nanofibers

ABSTRACT

The design, synthesis and photophysical properties of a Low Molecular Weight pH-responsive Gelator (LMWG) based on alkoxy group functionalized DCDHF-Hydrazones (DCDHF-H) are described. A straightforward synthesis of DCDHF-Hydrazone (DCDHF-H) chromophores was achieved via simple azo-coupling starting from 2-(dicyanomethylene)-2,5-dihydro-4,5,5-trimethylfuran-3-carbonitrile and alkoxy bearing aryl diazonium chloride derivatives. The DCDHF-H efficiently gelate selected organic solvents and reversibly respond to pH stimuli with a gel-sol conversion and an associated color change from yellow to purple. Self-assembly of these molecules, as indicated by X-ray crystallography, occurs via cooperative π - π stacking and van der Waals interactions producing gelation in some pure and mixed organic solvents. Furthermore, the presence of acidic or alkaline gases leads to a dramatic change in the rheological properties with potential applications in areas such as gas detection devices and drug release systems. Scanning electron microscopy (SEM) and transmission electron microscopy (TEM) studies of the xerogels obtained from *n*-propanol provide visual images revealing the formation of fibrous nanostructures.

Published by Elsevier Ltd.

1. Introduction

The distinctive ability of small organic gelators to immobilize organic solvents via the cooperative effects of weak non-covalent interactions such as hydrogen bonding, π - π stacking and van der Waals interactions, has received considerable interest. This interest extends more recently to their tunable physical properties and response to external stimuli [1–5]. This self-assembly in nanoscale supramolecular structures is likely to have significant implications in the creation of functional nanomaterials [6,7]. The types of supramolecular structures generated by these self-assembled fibrillar networks include nanofibers, nanorods, and nanoribbons. In order to create these assemblies, it is important to control the intermolecular interactions in such a way that the molecules can self-organize into fibrous higher order supramolecular structures but without conversion into a densified crystalline state [8–11].

Recently, stimuli-responsive low molecular weight gelators have been attracted attention due to their potential applications such as soft materials for drug delivery in the pharmaceutical industry, in the environmental area for capture and removal of pollutants and in reconstructive medicine for tissue engineering [12–17]. Low molecular weight pH-responsive gelators belong to a distinctive class in which variation of pH modulates a sol-gel phase transition. This behavior can be exploited to develop novel soft materials for encapsulation and slow release of biologically important molecules such as vitamins. Hence, it should be noted that development of stimuli-responsive smart gels is very appealing [11–20].

Many structure prototypes of low molecular weight organic gelators have been reported in the recent literature [6–10]. In contrast, only scant attention has been applied to the structures and properties of pH-responsive organogels. To the best of our knowledge, there is no report of low molecular weight organic gelators based on push-pull DCDHF chromophores. DCDHF derivatives have played a significant role in a range of recent advances of optoelectronic applications [21–25]. They have been intensively developed as photo- and electroluminescent materials in many

* Corresponding author. Department of Chemistry and Biochemistry, Kent State University, Kent, Ohio 44242, United States.

E-mail address: tkhattab@kent.edu (T.A. Khattab).

fields including electro-optics, photorefractives, single molecule fluorophores, dye lasers, fluorescent sensors and logic memory and organic light-emitting devices [26–30]. Therefore, the construction of an organogel based on DCDHF-H will be significant not only in the concept of designing new organogelators but also in extending gel-phase materials with appealing photonic and electronic functionality. We have found that long chain alkoxy substituted DCDHF-H derivatives can self-organize into supramolecular assemblies. Tuning the length of the alkoxy chain is instrumental for the fabrication of functional gels. Herein, we report the first example of pH-responsive low molecular weight organic gelator built from a solvatochromic and pH-responsive DCDHF-H molecular switch.

2. Experimental details

2.1. Apparatus

Melting points were obtained by differential scanning calorimetry (TA instruments 2920). Thermal stability was recorded by thermogravimetric analysis (TA instruments 2950). IR spectra were recorded with a Bruker Vectra-33 IR-Spectrometer with ATR probe. Elemental analyses (C, H, N) were performed on Perkin–Elmer 2400 analyzer (Perkin–Elmer, Norwalk, CT, USA) at the Microanalytical Center, Cairo University. UV–Vis absorption spectra were measured on a HP-8453 (HEWLETT PACKARD) spectrophotometer. Fluorescence spectra were measured on a VARIAN CARY ECLIPSE fluorescence spectrophotometer. NMR spectra were recorded using a BRUKER AVANCE 400 spectrometer at 400 MHz; chemical shifts are given in ppm relative to internal standard TMS at 295 K. The pH measurements were recorded with a BECKMAN COULTER digital pH340 pH meter, with a combined glass-calomel electrode. In case of scanning electron microscopy SEM, the gel formed from 5 in *n*-propanol was scooped up and placed on carbon tapes pasted on aluminum stubs and allowed to dry at room temperature in a desiccator connected to vacuum pump. The dried samples were then annealed overnight in an oven at 45 °C, followed by application of a 10 nm gold-coating before recording images. SEM images were obtained using Hitachi S-2600N operating at 20 kV. For Transmission electron microscopy TEM, a piece of gel 5 in *n*-propanol (at its minimum gelation concentration) was placed on a carbon-coated copper grid (200 mesh) and allowed to dry in vacuum at room temperature for two days. TEM was done on JEM-1200EX at an accelerating voltage of 80 kV. All materials and reagents were obtained from commercial sources and were used without further purification.

2.2. Materials and reagents

Solvents used in this study were obtained from Fluka and Aldrich. All reactions were monitored by thin layer chromatography (TLC) using Merck aluminum plates pre-coated with silica gel PF254; 20–20, 0.25 mm, and detected by visualization of the plate under UV lamp (1/4 254 or 365 nm). Compounds were purified through recrystallization or using flash column chromatography which was performed on Scharlau silica gel, packed by the slurry method. The DCDHF intermediate was prepared in a 68% yield according to an early literature method [25]. The starting material 2-amino-5-nitrophenol is commercially available and was treated with K₂CO₃ and 1-iodoalkane in dimethylformamide at reflux to afford the corresponding 2-alkyloxy-4-nitrobenzamine in relatively high yield range from 81 to 91% [31,32].

2.3. Gelation procedure

The gelation tests were performed by dissolution of compound 5

in *n*-propanol by heating at 85 °C and then cooling to room temperature to form the gel. The gels formed in 10–25 min depending on the gelator concentration. The gel melting temperature was determined by the inverted test tube method [8]. The vials containing the gels were kept upside down in a paraffin oil bath. The temperature was increased at a rate of 2 °C/min and the temperature at which the gel fell under gravity was recorded as the gel melting temperature.

2.4. Measurements of pH control

A solution of trifluoroacetic acid in methanol (conc. ca. 2×10^{-4} M) was added to either acetonitrile or ethanol solution of chromophore 5 (conc. ca. 3×10^{-6} M) to reduce the pH value. The hydrazone anions were produced in situ by addition of a base to solutions of their conjugate acids (DCDHF-H). For example, addition of a 1 M methanolic solution of tetrabutylammonium hydroxide to a solution of chromophore 5 in either acetonitrile or ethanol produced the corresponding hydrazone anion. The mixture was stirred and the pH values were recorded with a digital pH meter equipped with a combined glass-calomel electrode.

2.5. Procedure for concentration-dependent ¹H NMR measurements

The concentration-dependent ¹H NMR was carried out by gradually increasing the concentration of the CDCl₃ solution of DCDHF-H 5. The initial concentration of 5 is 0.7 mM, the concentration was then adjusted by direct addition of correct quantity of 5 into the CDCl₃ solution.

2.6. X-ray crystal structure information

Single crystals of compound 5 suitable for X-ray diffraction analysis were obtained by slow crystallization in a mixture of (EtOH/Toluene, 3:1). Crystal data were collected by mounting a crystal onto a thin glass fiber from a pool of Fluorolube™ and immediately placing it under a liquid N₂ cooled stream, on a Bruker AXS diffractometer upgraded with an APEX II CCD detector. The radiation used is graphite monochromatized Mo K α radiation ($\lambda = 0.7107$ Å). The lattice parameters are optimized from a least-squares calculation on carefully centered reflections. Lattice determination, data collection, structure refinement, scaling, and data reduction were carried out using APEX2 Version 2014.11 software package. The data were corrected for absorption using the SCALE program within the APEX2 software package. The structure was solved using direct methods. This procedure yielded a number of the C and N atoms. Subsequent Fourier synthesis yielded the remaining atom positions. The hydrogen atoms are fixed in positions of ideal geometry (riding model) and refined within the XSELL software package. These idealized hydrogen atoms had their isotropic temperature factors fixed at 1.2 or 1.5 times the equivalent isotropic U of the C atoms to which they were bonded. A few hydrogen atoms could not be adequately predicted via the riding model within the XSELL software. These hydrogen atoms were located via difference-Fourier mapping and subsequently refined. The final refinement of each compound included anisotropic thermal parameters on all non-hydrogen atoms. Crystallographic data (excluding structure factors) for the structure in this paper have been deposited with the Cambridge Crystallographic Data Centre as supplementary publication nos. CCDC 1443921. Copies of the data can be obtained, free of charge, via <http://pubs.acs.org> or on application to CCDC, 12 Union Road, Cambridge CB2 1EZ, UK, (Fax: +44 (0) 1223 336033 or e-mail: deposit@ccdc.cam.ac.uk).

2.7. Rheological measurements

Rheological examination was performed using a stress-controlled rheometer (TA Instruments, ARG2) equipped with steel parallel plate geometry (40 mm diameter), when the gap distance was set at 750 μm . All experiments were performed at 283 K. To determine the linear viscoelastic region (LVER) of the organogel sample, strain sweep at a constant frequency (6.28 rad/s) was achieved in the 0.05–200% range. The frequency sweep was conducted at a range of 0.1–100 rad/s at a constant strain of 0.1%, well within the linear regime determined by the strain sweep. In order to study the recovery performance of the gel, a thixotropic examination was performed. Just after the strain sweep progress, the recovery of the storage modulus G' of the cracked organogel was watched at a constant frequency (6.28 rad/s) under a low strain (0.1%). The storage modulus G' and the loss modulus G'' were recorded as functions of time in the recovery processes. To study the cycle of deformation and recovery, initially, a constant oscillatory strain (100%), that was enough to crack down the organogel, was applied to freshly prepared organogel for 10 s when the frequency of the measurement was 6.28 rad/s; then, the recovery of the storage modulus G' was observed at a constant frequency (6.28 rad/s) under a low strain (0.1%) within 20 s. Both G' and G'' were recorded as functions of time in each process.

3. Results and discussion

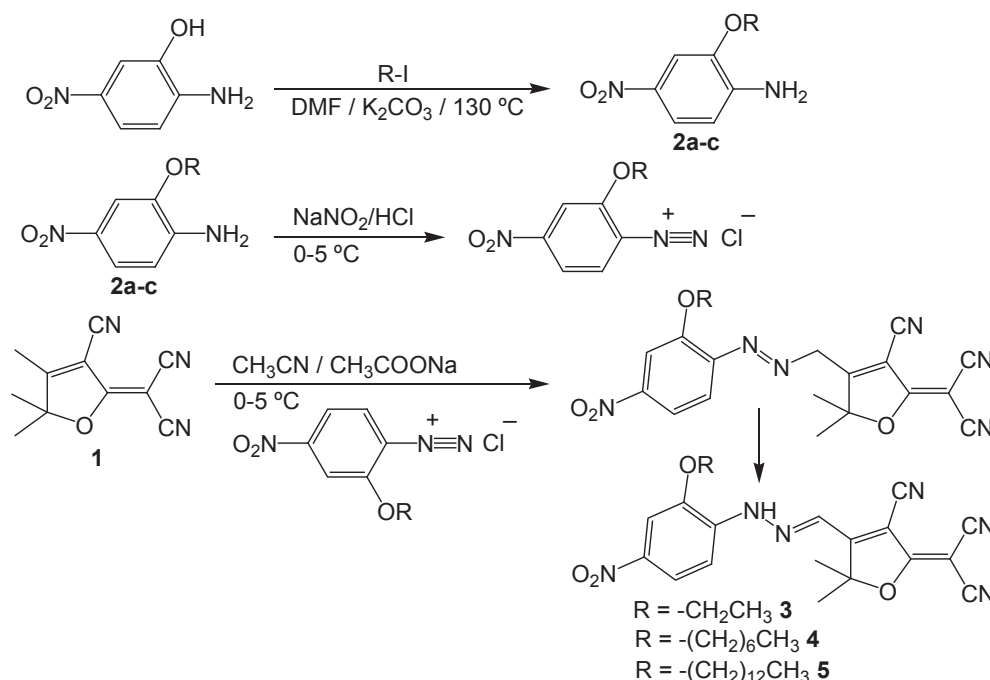
3.1. Synthesis and characterization

The simple synthetic approach utilized for the DCDHF-H chromophores are shown in Scheme 1 in which R represents an alkyl chain. The starting material 2-amino-5-nitrophenol is commercially available and was treated with K_2CO_3 and 1-iodoalkane in DMF at 130 °C to afford 2-alkyloxy-4-nitrobenzamine in high yield ranging from 81% to 91% [31,32]. The intermediate 2-(dicyanomethylene)-2,5-dihydro-4,5,5-trimethylfuran-3-carbonitrile **1** was prepared according to the literature method [25]. The

preparation of the DCDHF-H chromophores was simply performed via azo-coupling starting from 2-(dicyanomethylene)-2,5-dihydro-4,5,5-trimethylfuran-3-carbonitrile and diazonium salt derived from the corresponding 2-alkyloxy-4-nitrobenzamine [33]. The molecular structures of the produced chromophores 3–5 were characterized by ^1H - and ^{13}C -NMR spectroscopy, IR spectroscopy, elemental analysis, and X-ray crystal structure.

3.2. Photophysical properties of chromophores 3–5 in solution

The three colorants 3–5 are soluble in a range of both non-polar and polar organic solvents. All of the hydrazone chromophores show fluorescence emission in both polar and nonpolar solvents. Since the molecular frameworks of the chromophores 3–5 are very similar, they likewise have nearly identical absorption and emission behavior in solution. The UV–Vis absorption and fluorescence spectra of the hydrazone (H) and its corresponding hydrazone anion (HA) formed in some selected solvents are shown in Table 1. The colors of these DCDHF-H 3–5 in various pure solvents range from yellow to purple. In general, the main absorption peak undergoes a bathochromic shift (positive solvatochromism) with increasing solvent polarity (ca. 27 nm shift value for the hydrazone form and ca. 16 nm shift value for the hydrazone anion form on going from dichloromethane to dimethylsulfoxide); with diverse intensities. This indicates a strongly allowed π – π^* transition with charge transfer character. The DCDHF-H form showed interesting solvatofluorochromic property in various solvents as indicated in Table 1. The emission maximum of the neutral DCDHF-H dyes is shifted bathochromically as much as 25 nm while, in contrast, the DCDHF-H anion form did not show any fluorescence emission. When deprotonated, the entire hydrazone group can function as a bridge between donor and acceptor fragments in a push–pull system or function itself as a donor fragment when in conjugation with strong electron withdrawing group [34]. The 4-nitrophenylhydrazones possess an acidic N–H group, able to produce anions with an improved electron donating capability. Hence, distinct solvatochromic, solvatofluorochromic, and pH responsive



Scheme 1. Synthesis of chromophores 3–5.

Table 1
Optical properties in some selected solvents of the neutral hydrazone 5 (H form) and its corresponding deprotonated hydrazone anion (HA form) created in basic medium.

| Solvent | (H form) $\lambda_{\max, \text{abs.}}$ (nm); ϵ (molar absorptivity) $\text{L mol}^{-1} \text{cm}^{-1}$ | (H form) $\lambda_{\max, \text{em.}}$ (nm) | (HA form) $\lambda_{\max, \text{abs.}}$ (nm); ϵ (molar absorptivity) $\text{L mol}^{-1} \text{cm}^{-1}$ | (HA form) $\lambda_{\max, \text{em.}}$ (nm) |
|--------------------|---|--|--|---|
| Ethanol | 487 (59,793) | 534 | 560 (54,436) | – |
| <i>n</i> -Propanol | 489 (55,326) | 536 | 561 (61,589) | – |
| Acetonitrile | 477 (55,509) | 537 | 571 (66,124) | – |
| Dimethylsulfoxide | 498 (40,574) | 557 | 574 (73,678) | – |
| Dichloromethane | 471 (67,255) | 538 | 558 (64,678) | – |
| 1,4-Dioxane | 478 (67,255) | 532 | 570 (48,378) | – |

(–) No fluorescence activity noted.

activities were observed in polar protic and aprotic solvents.

3.3. pH-responsive molecular switching

The reversible sensing potential of the nitro-substituted DCDHF-H chromophores to undergo molecular switching imparted by pH stimulus was established by sequential addition of base and acid to a 3.0×10^{-6} M solution of DCDHF-H in either acetonitrile or ethanol. The reversible UV–Vis electronic absorption spectra and color switching changes of DCDHF-H 5 are shown in Fig. 1. The color evolves gradually from yellow, orange, orange-red, wine-red, violet, and purple at pH 5.38, 5.87, 6.21, 6.56, 6.78, and 7.04 respectively. Upon the addition of tetrabutylammonium hydroxide base to a solution of compound 5 in acetonitrile, the λ_{\max} at 477 nm decreased and a new peak at 571 nm appeared. The addition of trifluoroacetic acid produced reappearance of the absorption peak at 477 nm. Likewise, fluorescence emission intensity was varied, reversibly, at 537 nm in acetonitrile solution by the alternate addition of tetrabutylammonium hydroxide and trifluoroacetic acid as shown in Fig. 2 (excitation wavelength at 477 nm). Upon the addition of tetrabutylammonium hydroxide the fluorescence emission peak at 537 nm progressively decreases, while, in contrast, the intensity of the same peak increases with the addition of trifluoroacetic acid.

The stepwise addition of the tetrabutylammonium hydroxide base to a solution of 5 and subsequent recording of the corresponding absorption maxima λ_{\max} in acetonitrile led to a series of spectra with one isosbestic point at 516 nm (Fig. 1a). As a result of hydrazone anion formation, the intensity of the absorption at shorter wavelength (ca. 477 nm) decreased while simultaneous longer wavelength (ca. 571 nm) absorption appeared and grew in intensity. These results suggest that a strong quinoid-type interaction exists between the 4-nitrophenyl group and the lone-pair electrons on the secondary amine nitrogen atom in the hydrazone fragment, while such an extra resonance effect is depressed in the hydrazone anion presumably because the negative charge interacts instead more strongly to the strong DCDHF acceptor fragment (Scheme 2). Interestingly, UV–Vis absorption spectra of 5 in protic solvents (such as ethanol) display a series of spectra with two isosbestic points at 391 nm and 521 nm (Fig. 1b). One explanation for this additional isosbestic point appearing in protic solvents involves hydrogen bonding between the hydrazone anion and ethanol as the band at 273 nm increases with increasing the corresponding hydrazone anion band at 560 nm. The hydrogen bonding between the produced hydrazone anion and ethanol leads to a new species in equilibrium with other two species; the hydrazone dye and its corresponding hydrazone anion form

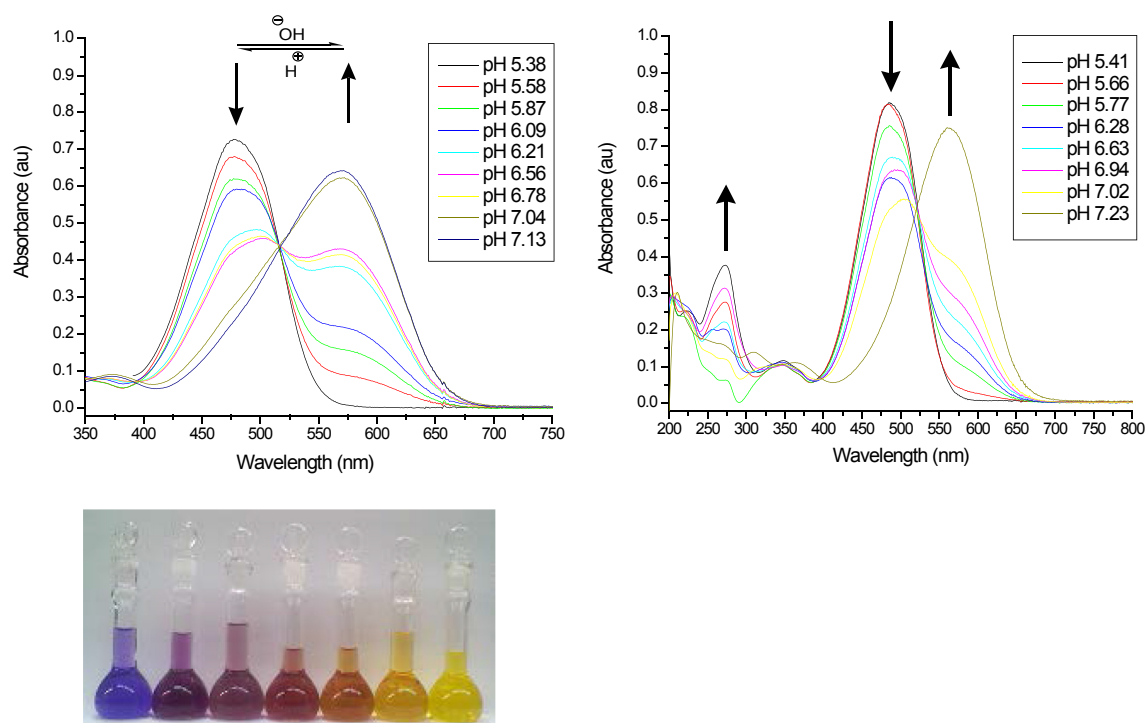


Fig. 1. The pH dependent absorption spectra of DCDHF-H 5 in acetonitrile (a) or ethanol (b) solutions (conc. 3.0×10^{-6} mol L^{-1}) at different pH values at ambient temperature.

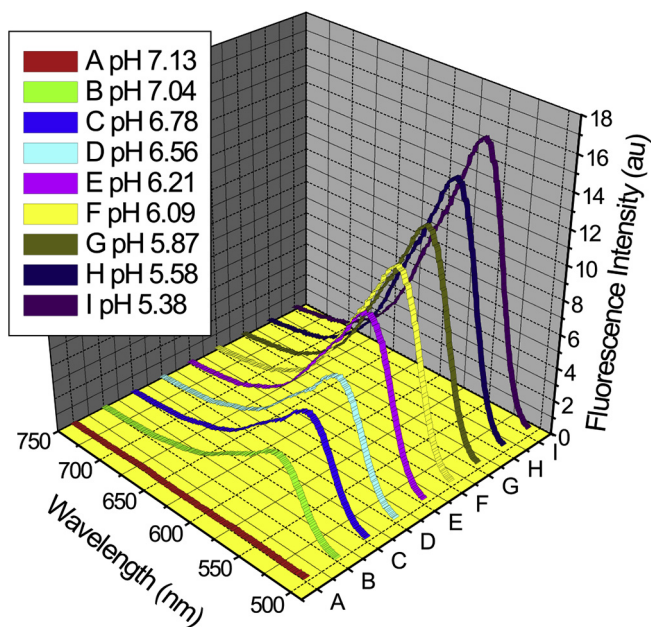
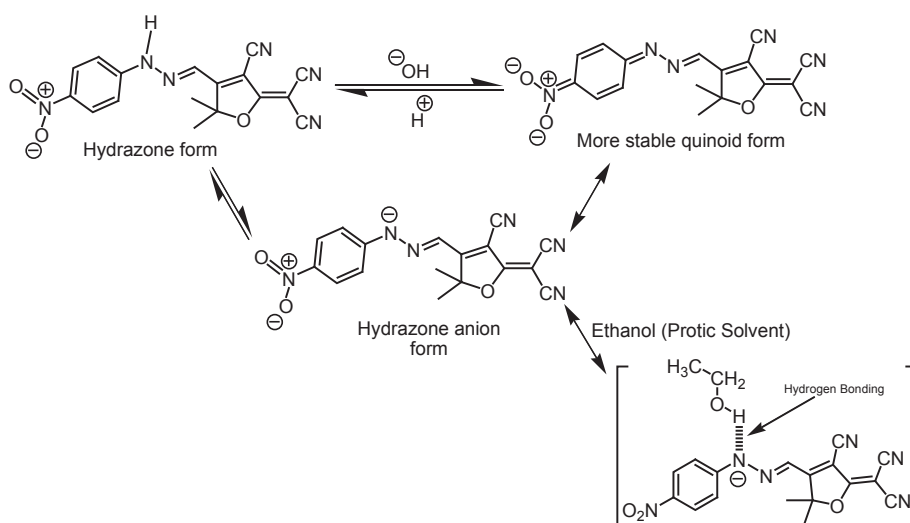


Fig. 2. Fluorescence emission of compound 5 in acetonitrile solution (conc. $3.0 \times 10^{-6} \text{ mol L}^{-1}$) at different pH values (ambient temperature, excitation wavelength at 477 nm).

(Scheme 2).

3.4. Gelation properties

The gelation properties of 3–5 were tested in various solvents by means of the “stable to inversion” technique [8]. It was found that both 3 and 4 did not form a gel following typical heating-cooling processes in any of the tested solvents which included cyclohexane, hexane, chloroform, tetrahydrofuran, ethanol, *tert*-butanol as well as some mixed solvents. Likewise, 5 did not form a gel in tetrahydrofuran, acetonitrile, chloroform, ethylacetate or dimethylsulfoxide in which the solubility was too high. Likewise, 5 could not gel in hexane or cyclohexane due to poor solubility.



Scheme 2. The pH of the environment has a dramatic influence on the electronic properties of the dyes and their respective absorption wavelengths. The hydrogen bonding between the hydrazone anion and ethanol leads to a new species in equilibrium with the other two species; namely, the hydrazone dye and its corresponding hydrazone anion form.

Table 2
Gelation properties of DCDHF-H 3–5 in different solvents.

| Solvent | 3 and 4 | 5 |
|---|---------|-------------|
| Ethanol | P | P |
| <i>n</i> -Propanol | P | G (2.24 mM) |
| <i>iso</i> -Propanol | P | P |
| <i>tert</i> -Butanol | P | P |
| <i>n</i> -Octanol | P | G (2.71 mM) |
| 1,2-Dihydroxyethane | P | G (3.68 mM) |
| 1,3-Dihydroxypropane | P | G (2.07 mM) |
| 1,6-Dihydroxyhexane | P | G (1.94 mM) |
| Benzyl alcohol | P | P |
| Benzene | I | I |
| Toluene | P | P |
| Hexane | I | I |
| Cyclohexane | I | I |
| Cyclohexane/chloroform (v/v = 2/3) | P | G (5.18 mM) |
| Chloroform | S | S |
| Acetone | S | S |
| Ethylacetate | S | S |
| Acetonitrile | S | S |
| THF | S | S |
| Dimethylformamide | S | S |
| Dimethylsulfoxide | S | S |
| Dimethylsulfoxide/cyclohexane (v/v = 1/2) | P | G (7.42 mM) |

G: gel; S: soluble; I: insoluble; P: precipitation. The critical gelation concentration (mM) is shown in parenthesis.

However, 5 does act as a gelator in pure alcoholic solvents. A series of mixed non-alcoholic solvents were also examined. It was found that an organogel of 5 could be generated in some mixed solvents such as chloroform/cyclohexane (v/v = 2/3) and dimethylsulfoxide/cyclohexane (v/v = 1/2). The results of the gelation studies are summarized in Table 2. The critical gelation concentration values were solvent dependent and in the range of 1.9 and 7.4 mM. Moreover, we found that the *n*-propanol gel and 1,3-propanediol gel formed from the DCDHF-H gelator 5 was stable for several weeks at room temperature, while under similar conditions the chloroform/cyclohexane gel could be preserved for only several days. The above results demonstrate the important role of the side chain in the gelation ability. The alkoxy side chain of 5 increases its solubility in a variety of solvents. Thus, the strong solvation of the alkoxy chain probably reduces any intermolecular affinity required

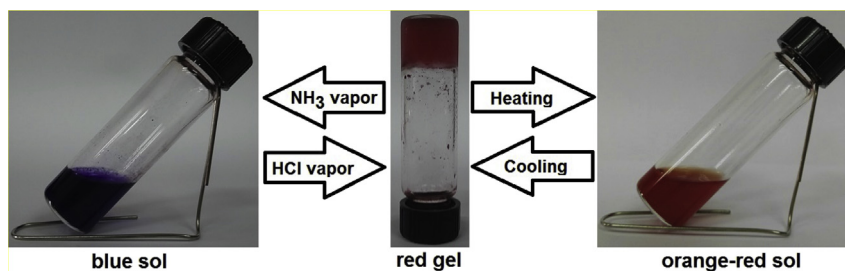


Fig. 3. Illustration of acid stability and base instability of the organogel of 5 in *n*-propanol.

for self-assembly. As compared with the gelation properties of 3 and 4, the long alkoxy chains are necessary features on the aromatic core for creating a good gelator. Indeed, decreasing the length of the alkoxy chain eliminates the gelation ability from 5 as indicated by compounds 3 and 4.

Interestingly, it is only the neutral hydrazone form that has any propensity for organogelation. Compound 5 was found to be a non-gelator in its hydrazone anion form in all solvents examined, whereas when it is used as its hydrazone form it formed strong gels in a subset of the solvents as discussed above. To illustrate the acid/base switching of this gel, a simple experiment was devised to show the reversible switching from gel \rightarrow sol \rightarrow gel of 5 in *n*-

propanol. Upon exposure to ammonia vapor, the initial gel of 5 (Fig. 3) formed a solution (this solution did not form a gel on subsequent heating or cooling) with a concomitant color change from orange to purple. When this purple solution was exposed to, the less toxic and volatile hydroiodic acid, hydrogen iodide vapor (long exposure), the gel was reformed (heating is required to re-produce the hydrazone form and the gel formed upon cooling to room temperature); with the color turning back to orange. Moreover, DCDHF-H 5 cannot gelate any of the organic solvents examined at/below pH 5.86. From the photophysical properties explained above, it is important to note that chromophore 5 turns orange in *n*-propanol at/below pH 5.77 and purple at/above pH 6.94.

From these results, we conclude that the gel is highly stable around the pH range 5.77–6.94. When the pH is lowered below 5.77 or higher above 6.94, the gel starts breaking slowly and completely breaks at pH 7.12 and at that pH the DCDHF-H 5 is

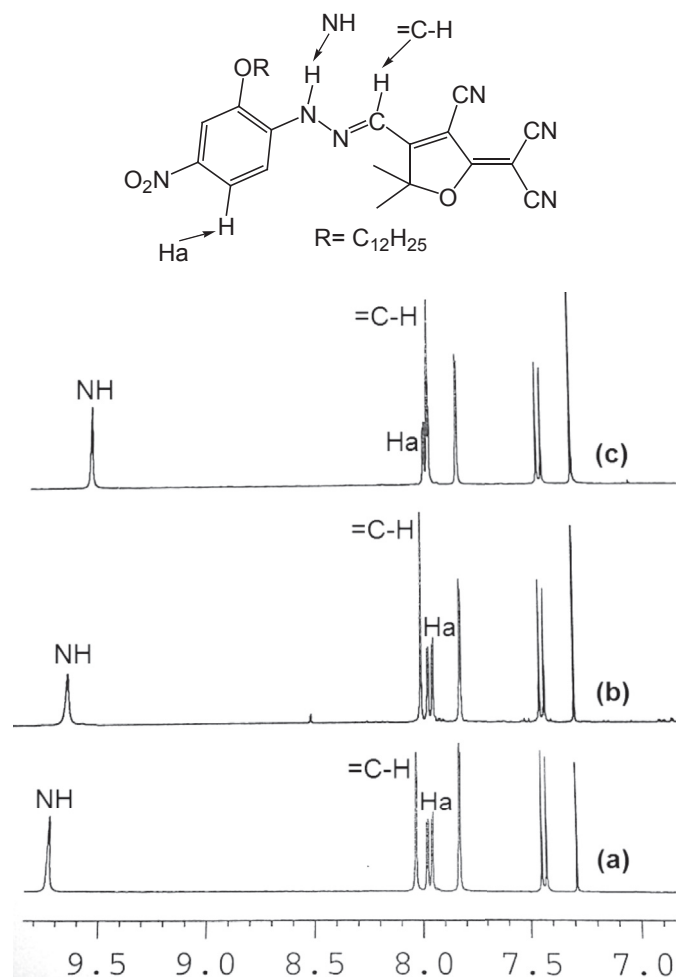
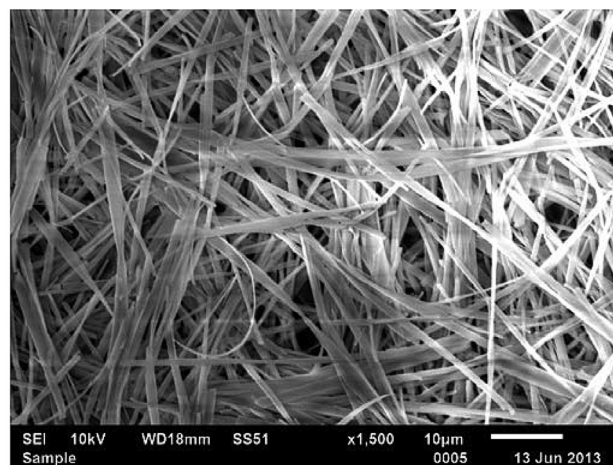
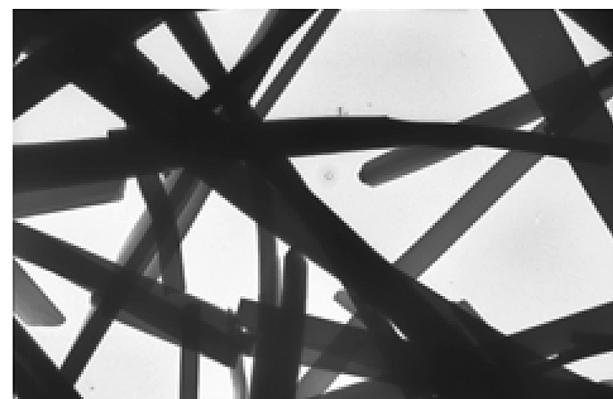


Fig. 4. Partial ^1H NMR spectra of DCDHF-H 5 in CDCl_3 at different concentrations (a) 1.74 mM; (b) 8.54 mM; and (c) 16.43 mM.



a.



b.

Fig. 5. SEM (a) and TEM (b) images for the dried xerogel of 5 obtained from *n*-propanol (2.24 mM).

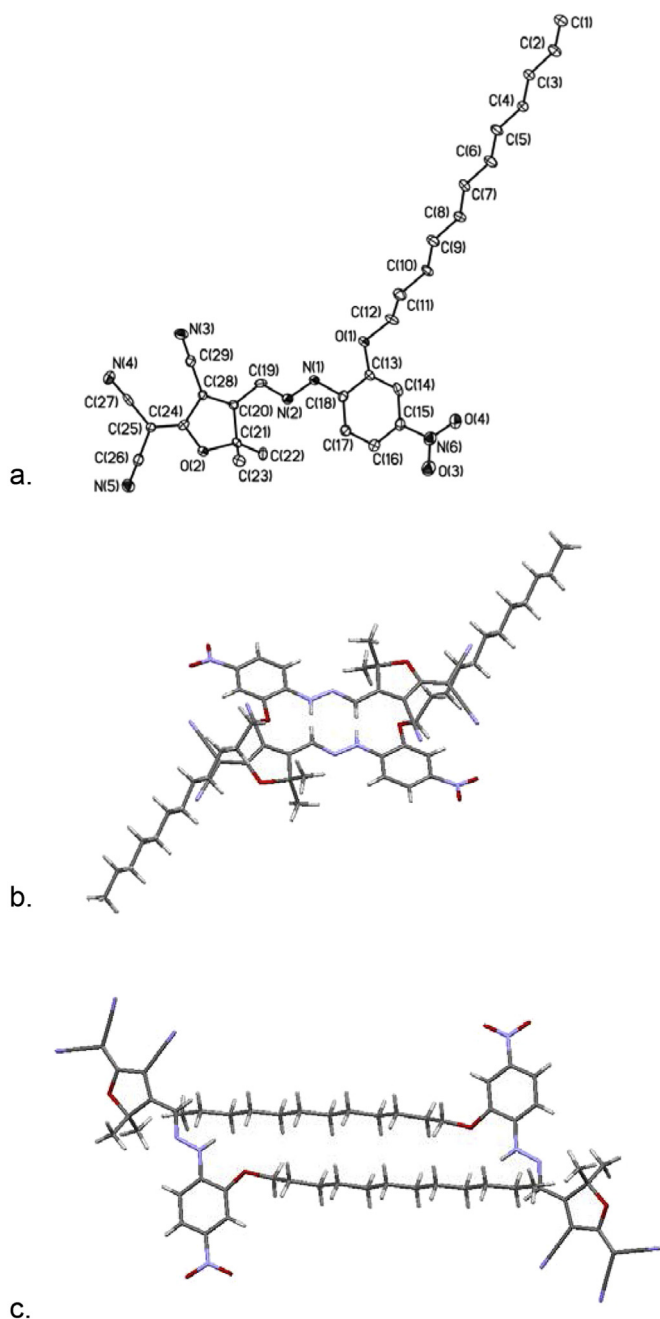


Fig. 6. (a) Crystal structure (ORTEP view) of 5 as derives from the X-ray analysis (thermal ellipsoid plots are drawn at the 30% probability level); (b) Face-to-face intermolecular π - π stacking interactions of the aromatic core; (c) Tail-to-tail van der Waals interactions between the alkoxy chains.

entirely precipitated out into two phases, the solid phase and the solution phase. At the higher pH > 6.94; the acidic hydrazone NH group is ionized inducing the gel to sol switch. However, at the lower pH < 6.94 (but higher than pH 5.77) the hydrazone group are protonated and this reduces the solubility and the gel-formation tendency of the DCDHF-H gelator 5 increases to a great extent. On the other hand, the same explanation can be applied when the pH is lowered below 5.77; as this leads to higher solubility of DCDHF-H 5 resulting in gel instability.

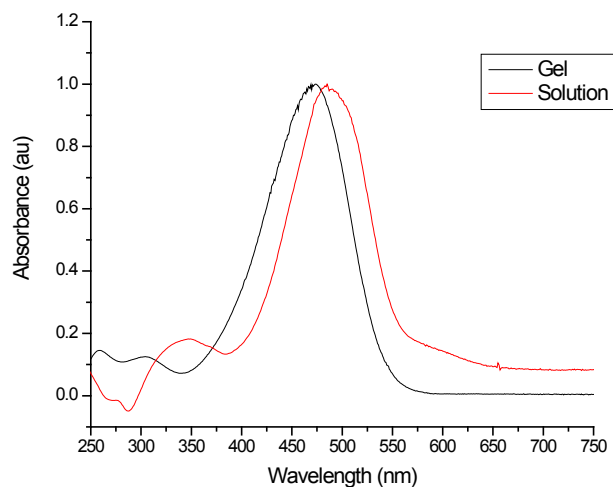


Fig. 7. Normalized UV/Vis absorption spectra of 5 in solution (red, 3.0×10^{-6} M) and in gel (black) in *n*-propanol. (For interpretation of the references to color in this figure legend, the reader is referred to the web version of this article.)

3.5. Morphology and structure of assemblies

It was observed that the long alkoxy chain of the DCDHF-H gelator 5 improves its solubility in organic solvents but also supports association between the fibers, via van der Waals forces, and eventual organogel formation. Therefore, of all the DCDHF-H gelators 3, 4, and 5, only the DCDHF-H 5 forms organogels with thixotropic property. It indicated that the long chain alkoxy group played an important role in the thixotropy of organogels. In the concentration-dependent ^1H NMR as shown in Fig. 4, the N-H resonance signals showed apparent downfield shifts as the concentration of 5 increased. These results revealed that the N-H groups formed hydrogen bonds in the gelation process. Similar behavior was monitored for the aliphatic =C-H resonance signals displayed apparent downfield shifts as the concentration of 5 increased. Furthermore, with the regular increase of concentration, the ^1H NMR signal of aryl rings (Ha) showed slight upfield shift, suggesting that the π - π stacking interactions among the aryl rings were involved in the gelation process.

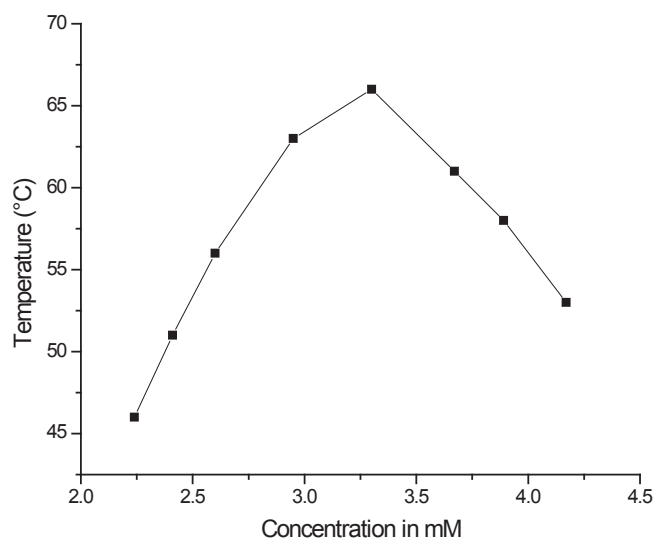


Fig. 8. Gel melting profile of gelator 5 in *n*-propanol at fixed pH 6.5.

The morphology of the *n*-propanol xerogel of compound 5 (after complete evaporation of the solvent) was studied by scanning electron microscopy and transmission electron microscopy. From the SEM and TEM images, we find a three-dimensional network consisting of many entangled fine fibers with diameters ranging from 220 nm to 1.2 μm as indicated by Fig. 5. This structure of the xerogel clearly shows the three-dimensional networks formed by the intertwined fibers that become swollen with immobilized organic solvent and results in the formation of the gels. Interestingly, the xerogel film responds reversibly to alkaline vapors with a concomitant color change from orange to blue. Therefore, these nanofibers may exhibit higher sensitivity in the detection of alkaline analytes due to the higher ratio of surface-to-volume, and the larger interspaces in the networks facilitates the convenient diffusion of guest gas molecules across the matrix. Therefore, the three dimensional networks based on xerogel from DCDHF-H 5 exhibit an efficient sensing ability (see video abstract). It is anticipated that the xerogel detection film can be employed for detection of toxic and invisible industrial gases such as ammonia used in industry especially refrigeration.

Supplementary video related to this article can be found at <http://dx.doi.org/10.1016/j.dyepig.2016.03.044>.

To understand the molecular structure and crystal packing, we obtained a single crystal of compound 5 from a mixture of ethanol/toluene (3:1) and subjected it to X-ray crystallography. The molecular structure in the crystal and the crystal packing structures of 5 are illustrated in Fig. 6. The crystal structure reveals two

molecules packed into H-aggregate in each unit cell, which was confirmed by the blue shift of the absorption of DCDHF-H 5 gel phase compared with that in dilute solution as shown in Fig. 7. In the crystal, each molecule interacts with the adjacent molecules in face-to-face intermolecular π - π stacking interactions of the aromatic core in cooperation with tail-to-tail van der Waals interactions between the alkoxy chains. The investigation of the crystal structure of 5 suggests that molecules should have the tendency to aggregate into two dimensional nanostructures.

The thermal stability of the organogel 5 in *n*-propanol was investigated by measuring the concentration dependent gel \rightarrow sol transition temperature at constant pH 6.5; as shown in Fig. 8. The results indicate that cooled organogel melting temperature increases within the temperature range 46–66 $^{\circ}\text{C}$ with increasing the gelator concentration from 2.24 to 3.30 mM. However, the organogel melting temperature was found to decrease with further increase of the gelator concentration (gelator concentration >3.30 mM). The reason for the decrease of thermal stability at gelator concentration >3.30 mM is not clearly understood. The increasing thermal stability at the gelator concentration range from 2.24 to 3.30 mM; can be attributed to the incorporation of a higher number of gelator molecules in the aggregate. In other words, increasing the gel \rightarrow sol transition temperature is associated with the growth of one-dimensional aggregates (nanofibers), which makes them more flexible, causing more entanglement of the fibers, and thereby increasing the transition temperature value.

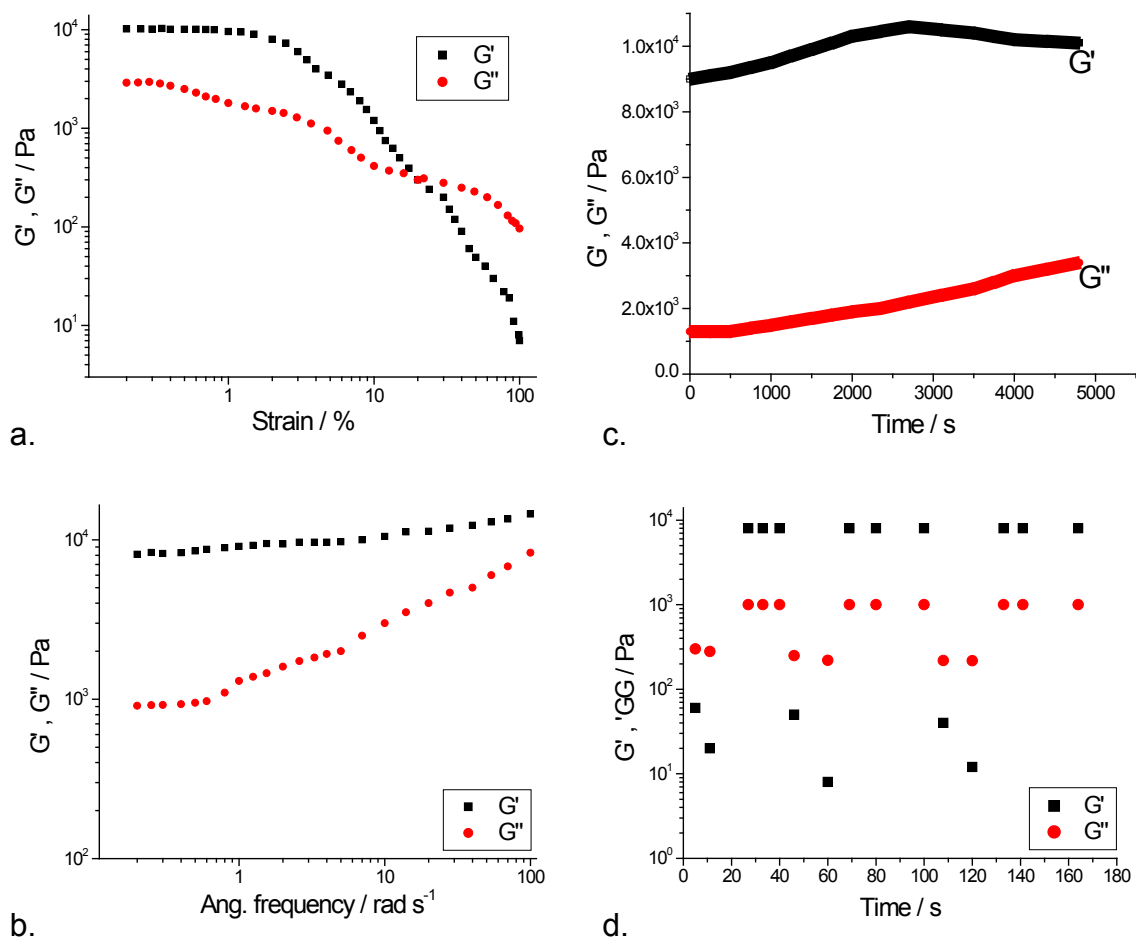


Fig. 9. Storage modulus G' and loss modulus G'' values of the organogel of 5 (2.24 mM) in *n*-propanol on the rheological experiments of (a) strain sweep; (b) Frequency sweep; (c) time sweep; and (d) three cycles of deformation and recovery processes.

3.6. Examination of thixotropic properties via rheological techniques

Of all the gels from homologous DCDHF-H gelators, only DCDHF-H 5 organogels exhibited the thixotropic property (Table 2). We found that the organogel of 5 in *n*-propanol exhibits thixotropic properties (Fig. 3). The organogel of 5 in *n*-propanol was changed to a solution by exposing to ammonia (alkaline) gas, and then regenerated rapidly with acidic (HCl) vapor. This reversible gel-sol phase transition could be repeated many times. To the best of our knowledge, there is no reported example of a thixotropic DCDHF-Hydrazone organogel. Rheological characterizations of organogels were additionally achieved in dynamic manner to examine this pH-responsive behavior in detail. Although the alkaline ammonia gas broke the well-established assemblies, the acidic vapors lead to reformation of organogel while it retained the thixotropic properties. The rheological experiments on the organogel of 5 in *n*-propanol were then conducted. The variations in storage modulus (G') and loss modulus (G'') under shear strain were recorded (Fig. 9a). At low strain values, the G' values are one order of magnitude larger than those of G'' , suggesting the dominant elastic nature of the organogel. Both G' and G'' continue roughly constant below the critical strain value (ca. 1.0%). When the strain value is above 1.0%, both G' and G'' regularly reduced, indicating a partial breakup of the organogel. The changes of storage modulus (G') and loss modulus (G'') as a function of angular frequency were also determined as shown in Fig. 9b. The frequency sweep results also show that at low

frequency values (ca. below 1.0 rad/s), the G' values are one order of magnitude larger than the values of G'' , suggesting the performance of a “true gel”. However, both G' and G'' demonstrate apparent frequency dependency in the 1.0–100 rad/s frequency range, which indicates that the organogel has poor tolerance to external forces in the 1.0–100 rad/s frequency range. The recovery property of the organogel of 5 in *n*-propanol was further studied. As shown in Fig. 9c, after the gel is continually deformed at 100% deformation for 30 s, its G' and G'' are monitored over 5000 s to follow the structural recovery of the gel. The gel recovers its elastic character rapidly and proceeds as a gel-like material once the external force is removed. Furthermore, the thixotropic process of the gel is completely reproducible for at least three cycles as shown in Fig. 9d. Generally, the rheological measurements demonstrate that the organogel of 5 is a robust thixotropic gel with a fast-recovery ability, which might be attributed to the rapid reorganization of these molecules via cooperative π – π stacking and van der Waals interactions.

4. Conclusions

Three pH-responsive DCDHF dyes containing a hydrazone unit as part of the π -system have been successfully designed, synthesized and characterized. We have demonstrated an interesting protonation and deprotonation induced gelation of a DCDHF-H gelator. It was possible to demonstrate the acid stability and base instability of the obtained organogel. It was also found that the organogels showed high thermal stability and their morphology was fibers of diameters ranging from 220 nm to 1.2 μ m. This low molecular weight gelator, that can gelate organic solvents, represents a new class of gelators that have the ability to respond to acid/base stimuli and are potentially valuable in emerging fields. Compound 5 can assemble to form the molecular stacks in solution; however, further stacking to generate the supramolecular morphology needs the support of van der Waals interactions of the long alkoxy chain. Although the organogel is quite stable in the presence of alcohol, the gelation properties can be modulated by

changing the pH value. These organogels in different pH media have melting temperatures higher than the physiological temperature. Thus the DCDHF-H organogel may have potential application in drug delivery.

Acknowledgments

This research was supported by the National Science Foundation through the Center for Layered Polymer Systems (CLiPS) under Grant No. 0423914. This material was also supported by the USDA grant # 58-3148-2-113.

Appendix A. Supplementary data

Supplementary data related to this article can be found at <http://dx.doi.org/10.1016/j.dyepig.2016.03.044>.

References

- [1] An Byeong-Kwan, Lee Deug-Sang, Lee Jong-Soon, Park Yil-Sung, Song Hyung-Su, Park Soo Young. Strongly fluorescent organogel system comprising fibrillar self-assembly of a trifluoromethyl-based cyanostilbene derivative. *J Am Chem Soc* 2004;126(33):10232–3.
- [2] Tsou Chia-Chen, Sun Shih-Sheng. New fluorescent amide-functionalized phenylethynylthiophene low molecular weight gelator. *Org Lett* 2006;8(3):387–90.
- [3] Wang Sisi, Xue Pengchong, Wang Panpan, Yao Boqi, Li Kechang, Liu Baijun. Fluorescence-enhanced gels of D- π -A diphenylacrylonitrile derivatives: influence of nitro group and alkoxy chain. *Dyes Pigments* 2015;122:302–9.
- [4] Li Xue-Qing, Stepanenko Vladimir, Chen Zhijian, Prins Paulette, Siebbeles Laurens DA, Würthner Frank. Functional organogels from highly efficient organogelator based on perylene bisimide semiconductor. *Chem Commun* 2006;37:3871–3.
- [5] Jeong Yeonhwan, Hanabusa Kenji, Masunaga Hiroyasu, Akiba Isamu, Miyoshi Kentaro, Sakurai Shinichi, et al. Solvent/gelator interactions and supramolecular structure of gel fibers in cyclic bis-urea/primary alcohol organogels. *Langmuir* 2005;21(2):586–94.
- [6] Zhang Xiaofei, Lu Ran, Jia Junhui, Liu Xingliang, Xue Pengchong, Xu Defang, et al. Organogel based on β -diketone-boron difluoride without alkyl chain and H-bonding unit directed by optimally balanced π – π interaction. *Chem Commun* 2010;46(44):8419–21.
- [7] He Yabing, Bian Zheng, Kang Chuanqing, Cheng Yanqin, Gao Lianxun. Novel C 3-symmetrical triphenylbenzene-based organogelators with different linkers between phenyl ring and alkyl chain. *Tetrahedron* 2010;66(19):3553–63.
- [8] Wang Xiao-Jun, Xing Ling-Bao, Cao Wei-Ning, Li Xu-Bing, Chen Bin, Tung Chen-Ho, et al. Organogelators based on TTF supramolecular assemblies: synthesis, characterization, and conductive property. *Langmuir* 2010;27(2):774–81.
- [9] Xue Pengchong, Lu Ran, Chen Guojun, Zhang Yuan, Nomoto Hiroyuki, Takafuji Makoto, et al. Functional organogel based on a salicylideneaniline derivative with enhanced fluorescence emission and photochromism. *Chem A Eur J* 2007;13(29):8231–9.
- [10] Yoshida Masaru, Koumura Nagatoshi, Misawa Yoshihiro, Tamaoki Nobuyuki, Matsumoto Hajime, Kawanami Hajime, et al. Oligomeric electrolyte as a multifunctional gelator. *J Am Chem Soc* 2007;129(36):11039–41.
- [11] Sangeetha Neralagatta M, Maitra Uday. Supramolecular gels: functions and uses. *Chem Soc Rev* 2005;34(10):821–36.
- [12] Ray Sudipta, Das Apurba K, Banerjee Arindam. pH-responsive, bolaamphiphile-based smart metallo-hydrogels as potential dye-adsorbing agents, water purifier, and vitamin B12 carrier. *Chem Mater* 2007;19(7):1633–9.
- [13] Miao Wangen, Qin Long, Yang Dong, Jin Xue, Liu Minghua. Multiple-stimulus-responsive supramolecular gels of two components and dual chiroptical switches. *Chem A Eur J* 2015;21(3):1064–72.
- [14] Kim Sung-Hoon, Hwang In-Jeong, Gwon Seon-Yeong, Son Young-A. The thermoresponsive behaviour of a poly (N-isopropylacrylamide) hydrogel with a D- π -A type pyran-based fluorescent dye. *Dyes Pigments* 2010;87(1):84–8.
- [15] Cornwell Daniel J, Smith David K. Expanding the scope of gels—combining polymers with low-molecular-weight gelators to yield modified self-assembling smart materials with high-tech applications. *Mater Horiz* 2015;2(3):279–93.
- [16] Kim Tae Hyeon, Kim Dai Geun, Lee Minjung, Lee Taek Seung. Synthesis of reversible fluorescent organogel containing 2-(2'-hydroxyphenyl) benzoxazole: fluorescence enhancement upon gelation and detecting property for nerve gas simulant. *Tetrahedron* 2010;66(9):1667–72.
- [17] Guan Xidong, Fan Kaiqi, Gao Tongyang, Ma Anping, Zhang Bao, Song Jian. A novel multi-stimuli responsive gelator based on d-gluconic acetal and its potential applications. *Chem Commun* 2016;52(5):962–5.
- [18] Lin Qi, Zhu Xin, Fu Yong-Peng, Yang Qing-Ping, Sun Bin, Wei Tai-Bao, et al.

- Rationally designed supramolecular organogel dual-channel sense F⁻ under gel-gel states via ion-controlled AIE. *Dyes Pigments* 2015;113:748–53.
- [19] Arndt Karl-Fr, Schmidt Thomas, Richter Andreas, Kuckling Dirk. High response smart gels: synthesis and application. In: *Macromolecular Symposia*. Vol. 207. No. 1. WILEY-VCH Verlag; 2004.
- [20] Grove Tijana Z, Forster Jason, Pimienta Genaro, Dufresne Eric, Regan Lynne. A modular approach to the design of protein-based smart gels. *Biopolymers* 2012;97(7):508–17.
- [21] Lu Zhikuan, Lord Samuel J, Wang Hui, Moerner WE, Twieg Robert J. Long-wavelength analogue of PRODAN: synthesis and properties of Anthradan, a fluorophore with a 2, 6-donor-acceptor anthracene structure. *J Org Chem* 2006;71.26:9651–7.
- [22] Lord Samuel J, Lu Zhikuan, Wang Hui, Willets Katherine A, Schuck PJames, Lee Hsiao-lu D, et al. Photophysical properties of acene DCDHF fluorophores: long-wavelength single-molecule emitters designed for cellular imaging. *J Phys Chem A* 2007;111(37):8934–41.
- [23] Luo Jingdong, Zhou Xing-Hua, Jen Alex K-Y. Rational molecular design and supramolecular assembly of highly efficient organic electro-optic materials. *J Mater Chem* 2009;19(40):7410–24.
- [24] Lu Zhikuan, Liu Na, Lord Samuel J, Bunge Scott D, Moerner WE, Twieg Robert J. Bright, red single-molecule emitters: synthesis and properties of environmentally sensitive dicyanomethylenedihydrofuran (DCDHF) fluorophores with bisaromatic conjugation. *Chem Mater* 2009;21(5):797–810.
- [25] Davis Matthew C, Chafin Andrew P, Hollins Richard A, Baldwin Lawrence C, Erickson Eric D, Zarras Peter, et al. Synthesis of an isophorone-based nonlinear optical chromophore. *Synth Commun* 2004;34(18):3419–29.
- [26] Lee Marissa K, Williams Jarrod, Twieg Robert J, Rao Jianghong, Moerner WE. Enzymatic activation of nitro-aryl fluorogens in live bacterial cells for enzymatic turnover-activated localization microscopy. *Chem Sci* 2013;4(1):220–5.
- [27] Park Jeeseok, Kim Hyunjin, Choi Yongdoo, Kim Youngmi. A ratiometric fluorescent probe based on a BODIPY–DCDHF conjugate for the detection of hypochlorous acid in living cells. *Analyst* 2013;138(12):3368–71.
- [28] Willets Katherine A, Nishimura Stefanie Y, Schuck P James, Twieg Robert J, Moerner WE. Nonlinear optical chromophores as nanoscale emitters for single-molecule spectroscopy. *Acc Chem Res* 2005;38(7):549–56.
- [29] Cheng Yen-Ju, Luo Jingdong, Hau Steven, Bale Denise H, Kim Tae-Dong, Shi Zhengwei, et al. Large electro-optic activity and enhanced thermal stability from diarylaminophenyl-containing high- β nonlinear optical chromophores. *Chem Mater* 2007;19(5):1154–63.
- [30] Gubler Ulrich, He Meng, Wright Daniel, Roh Yeonsuk, Twieg Robert, Moerner WE. Monolithic photorefractive organic glasses with large coupling gain and strong beam fanning. *Adv Mater* 2002;14(4):313.
- [31] Su Bin, Diaz-Cruz Edgar S, Landini Serena, Bruggemeier Robert W. Novel sulfonanilide analogues suppress aromatase expression and activity in breast cancer cells independent of COX-2 inhibition. *J Med Chem* 2006;49(4):1413–9.
- [32] Su Bin, Chen Shiuan. Lead optimization of COX-2 inhibitor nimesulide analogs to overcome aromatase inhibitor resistance in breast cancer cells. *Bioorg Med Chem Lett* 2009;19.23:6733–5.
- [33] Khattab Tawfik A, Abdelmoez Sherif, Klapötke Thomas M. Electrospun nanofibers from a tricyanofuran-based molecular switch for colorimetric recognition of ammonia gas. *Chem A Eur J* 2016;22(12):4157–63.
- [34] Millán Daniela, Domínguez Moisés, Rezende Marcos Caroli. Solvatochromic hydrazone anions derived from chalcones. *Dyes Pigments* 2008;77(2):441–5.